

Histone hyperacetylation during meiosis interferes with large-scale chromatin remodeling, axial chromatid condensation and sister chromatid separation in the mammalian oocyte

FEIKUN YANG^{#,1}, CLAUDIA BAUMANN[#], MARIA M. VIVEIROS and RABINDRANATH DE LA FUENTE*

Department of Physiology and Pharmacology, College of Veterinary Medicine, University of Georgia, Athens, GA, USA

ABSTRACT Histone acetylation regulates higher-order chromatin structure and function and is critical for the control of gene expression. Histone deacetylase inhibitors (HDACi) are currently under investigation as novel cancer therapeutic drugs. Here, we show that female germ cells are extremely susceptible to chromatin changes induced by HDACi. Our results indicate that exposure to trichostatin A (TSA) at nanomolar levels interferes with major chromatin remodeling events in the mammalian oocyte leading to chromosome instability. High resolution analysis of chromatin structure and live-cell imaging revealed a striking euchromatin decondensation associated with histone H4 hyperacetylation following exposure to 15 nM TSA in >90% of pre-ovulatory oocytes. Dynamic changes in large-scale chromatin structure were detected after 2 h of exposure and result in the formation of misaligned chromosomes in >75% ($P<0.05$) of *in vitro* matured oocytes showing chromosome lagging as well as abnormal sister chromatid separation at anaphase I. Abnormal axial chromatid condensation during meiosis results in the formation of elongated chromosomes exhibiting hyperacetylation of histone H4 at lysine 5 and lysine 16 at interstitial chromosome segments, but not pericentric heterochromatin, while highly decondensed bivalents exhibit prominent histone H3 phosphorylation at centromeric domains. Notably, no changes were observed in the chromosomal localization of the condensin protein SMC4. These results indicate that HDAC activity is required for proper chromosome condensation in the mammalian oocyte and that HDACi may induce abnormal chromosome segregation by interfering with both chromosome-microtubule interactions, as well as sister chromatid separation. Thus, HDACi, proposed for cancer therapy, may disrupt the epigenetic status of female germ cells, predisposing oocytes to aneuploidy at previously unrecognized low doses.

KEY WORDS: *centromere, heterochromatin, chromatin remodeling, histone deacetylase, TSA epigenetic modifications, meiosis*

Introduction

Functional differentiation of chromatin structure during oocyte growth is essential for the acquisition of both meiotic and developmental potential in the mature female gamete (De La Fuente, 2006, Li, 2002, Patterton and Wolffe, 1996). Developmental transitions in large-scale chromatin structure are regulated through the establishment of multiple posttranslational modifications such as phosphorylation, acetylation and/or methylation at specific lysine residues predominantly of Histones H3/H4 (Kageyama *et al.*, 2007, Kota and Feil, 2010, Sarmiento *et al.*, 2004) and constitute an essential epigenetic mechanism for the control of nuclear architecture, transcriptional regulation and centromeric heterochromatin forma-

tion (Baumann *et al.*, 2010, De La Fuente, 2006).

Meiotic chromosomes exhibit unique functional and structural properties to ensure the proper segregation of homologous chromosomes at metaphase I and of sister chromatids following fertilization of metaphase II arrested oocytes (De La Fuente *et al.*, 2012, Petronczki *et al.*, 2003, Revenkova *et al.*, 2001). The unique functional properties of meiotic chromosomes require a series of germ-cell specific mechanisms for the control of chromatin remodeling in the germ line (De La Fuente, 2006, Kimmins and Sassone-Corsi, 2005, Kota and Feil, 2010, Li, 2002, Revenkova

Abbreviations used in this paper: GV, germinal vesicle; HDAC, histone deacetylase; HDACi, histone deacetylase inhibitor; TSA, trichostatin A.

*Address correspondence to: Rabindranath De La Fuente. Department of Physiology and Pharmacology, College of Veterinary Medicine, University of Georgia, 501 D.W. Brooks Drive, Athens, GA, 30602, USA. e-mail: rfuente@uga.edu

These authors contributed equally to this work. 1 Current address: Departments of Environmental Medicine and Pharmacology, New York University School of Medicine, Tuxedo, NY, USA.

Supplementary Material (one figure) for this paper is available at: <http://dx.doi.org/10.1387/ijdb.120246rd>

Final, author-corrected PDF published online: 5 February 2013.

et al., 2004). For example, fully-grown oocytes exhibit a striking large-scale chromatin remodeling event leading to the formation of a transcriptionally quiescent nuclear environment in preparation for accurate chromosome condensation and segregation during meiosis (Abe *et al.*, 2010, De La Fuente, 2006, De La Fuente and Eppig, 2001, De La Fuente *et al.*, 2004, Miyara, 2003, Wickramasinghe *et al.*, 1991, Zuccotti, 1995). As the growing oocyte acquires both meiotic and developmental competence, a decondensed and transcriptionally active nucleus that exhibits a characteristic non surrounded nucleolus (NSN) configuration is progressively remodeled into a condensed, transcriptionally quiescent chromatin state called the surrounded nucleolus (SN) configuration when centromeric satellite DNA forms a prominent heterochromatin rim around the nucleolus in a configuration that might be required for proper meiotic progression (Abe *et al.*, 2010, De La Fuente, 2006, De La Fuente and Eppig, 2001, De La Fuente *et al.*, 2004, Wickramasinghe *et al.*, 1991, Zuccotti, 1995).

In spite of the transcriptionally repressive chromatin environment

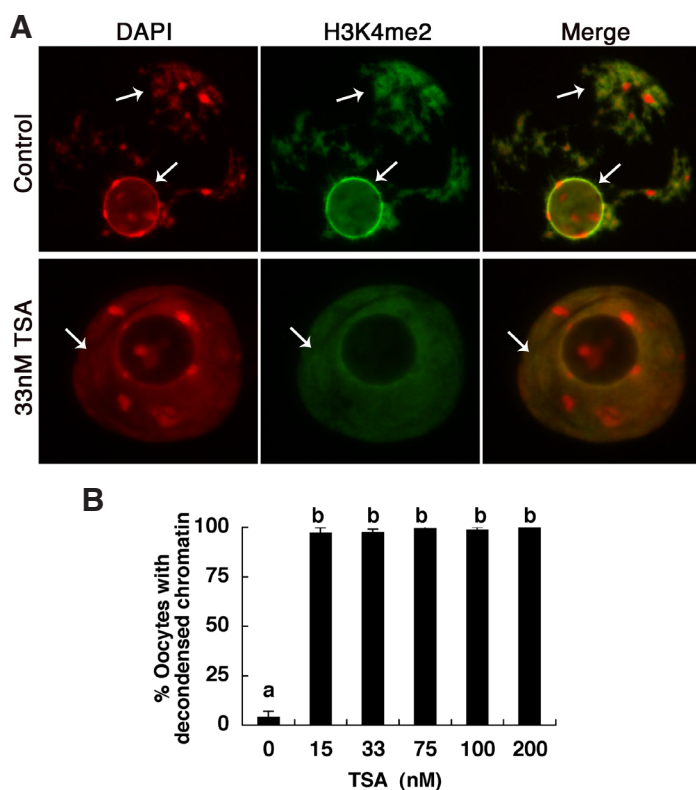


Fig. 1. Major chromatin remodeling is disrupted in germinal vesicle (GV) stage oocytes following 8 h of trichostatin A (TSA) treatment. (A) Untreated control GV oocytes (upper panel) showing a characteristic SN chromatin configuration (arrows; DAPI pseudo colored in red) following culture for 8 h. Histone H3 lysine 4 dimethylation (H3K4me2, green) demonstrates prominent signals at the perinucleolar chromatin rim, but is excluded from DAPI-bright heterochromatin domains. Treatment with 33 nM TSA during the culture period induced global chromatin decondensation and resulted in a redistribution of H3K4 dimethylation throughout the entire germinal vesicle (lower panel, arrow). **(B)** A significant increase ($P < 0.05$) in the proportion of oocytes showing extensive chromatin decondensation following TSA treatment was detectable with as low as 15 nM TSA and at all concentrations tested. Data are presented as the mean \pm SEM of three independent experimental replicates.

present in pre-ovulatory oocytes, acetylation of histone H3 and histone H4 can readily be detected at basal levels in the nucleus or germinal vesicle (GV) of pre-ovulatory oocytes (Adenot *et al.*, 1997, De La Fuente *et al.*, 2004). However, coincident with the onset of meiotic resumption and GV breakdown, a wave of global histone deacetylation removes the majority of acetylated histone marks throughout the entire length of the condensing chromatids of meiotic bivalents in a process that is critical for proper chromosome condensation, the recruitment of centromeric proteins such as ATRX and the establishment of specialized chromosome-microtubule interactions in mammalian oocytes (De La Fuente, 2006, De La Fuente *et al.*, 2004, De La Fuente *et al.*, 2004, Kim *et al.*, 2003). Although the molecular mechanisms involved in the large scale remodeling of specific histone residues from meiotic chromosomes are not known, exposure of mammalian oocytes to the histone deacetylase inhibitor trichostatin A (TSA) prevents the onset of global deacetylation and induces the formation of hyperacetylated chromosomes that exhibit abnormal chromosome condensation and improper attachment to the microtubular network (Akiyama *et al.*, 2006, De La Fuente, 2006, De La Fuente *et al.*, 2004).

Histone deacetylases (HDAC1 and HDAC2) are essential for oocyte growth and survival beyond the secondary follicle stage (Ma *et al.*, 2012). Moreover, accumulating evidence indicates that global histone deacetylation during meiotic resumption is critical for the maintenance of chromosome stability in the female gamete as demonstrated by the high levels of chromosome segregation defects observed in mammalian oocytes following transient exposure to TSA (De La Fuente, 2006, De La Fuente *et al.*, 2004) as well as the transmission of an aneuploid chromosome complement to the early conceptus following fertilization (Akiyama *et al.*, 2006). Notably, >80% of metaphase I and metaphase II stage human oocytes obtained from women of advanced reproductive age exhibited persistence of histone H4 acetylation at lysine 12 (H4K12) associated with misaligned chromosomes. Thus, abnormal regulation of histone deacetylases (HDACs) and the subsequent lack of global histone deacetylation during oocyte aging might also be an important mechanism contributing to the high rates of aneuploidy observed in human oocytes during advanced maternal age (van den Berg *et al.*, 2011).

Studies suggest that global histone deacetylation during meiosis might be an essential mechanism to recruit large protein complexes essential for chromosome condensation, the regulation of centromeric heterochromatin formation, and the epigenetic control of centromere function (Akiyama *et al.*, 2006, De La Fuente, 2006, De La Fuente *et al.*, 2004). Notably, this mechanism seems to be particularly susceptible to environmental or pharmacological disruption in the mammalian oocyte. For example, somatic cells require a prolonged treatment of at least 5 days with 100 ng/ml TSA during which, inhibition of HDACs results in lack of recruitment of heterochromatin protein 1 (HP1 β) to centromeric domains and the progressive appearance of abnormal chromosome segregation defects during mitosis (Taddei *et al.*, 2001, Taddei *et al.*, 2005). In contrast, TSA induced chromosome-wide hyperacetylation and interfered with recruitment of ATRX to centromeric domains within 8 hours of exposure resulting in the presence of chromosomal non-disjunction in >60% of metaphase II stage oocytes (De La Fuente, 2006, De La Fuente *et al.*, 2004) and leading to the transmission of aneuploidy and subsequent post-implantation embryo loss (Akiyama *et al.*, 2006).

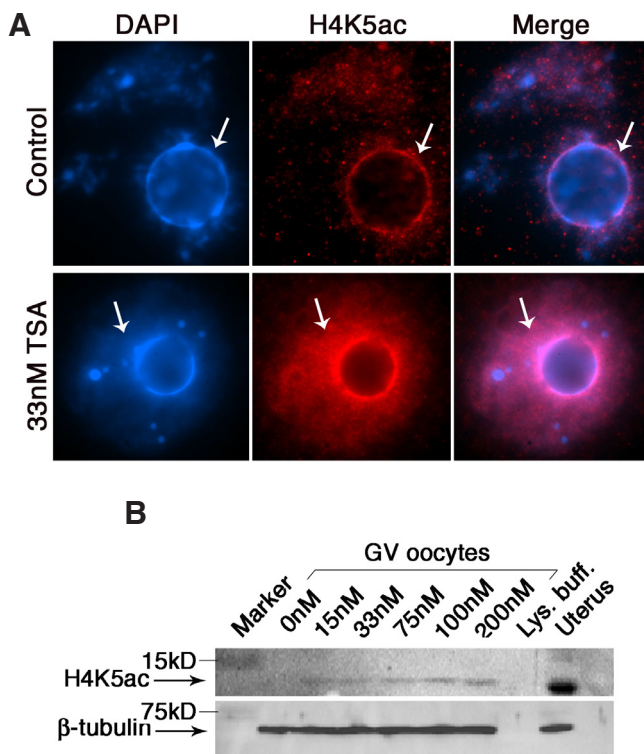


Fig. 2. Exposure of pre-ovulatory oocytes to trichostatin A (TSA) induces histone hyperacetylation at nanomolar concentrations. (A) Oocytes were maintained at the GV stage for 8 h in the presence or absence of TSA. In control oocytes, acetylation of lysine 5 in histone H4 (H4K5ac, red) is detectable at basal levels confined to the chromatin domains surrounding the nucleolus (arrow) as well as relatively compact chromatin clusters. TSA treatment induced global chromatin decondensation (blue) and hyperacetylation of H4K5ac throughout the nucleus (arrow). (B) Western blot analysis revealed an H4K5ac-immunoreactive band with a molecular weight of approximately 13 kDa in all treatment groups (15 to 200 nM). In contrast, in control oocytes (0 nM), basal levels of H4K5ac were undetectable, further demonstrating hyperacetylation in TSA-treated GV oocytes. No changes were observed in the total protein levels of β -tubulin used as a loading control. Lys. Buff., lysis buffer control.

Histone deacetylase inhibitors (HDACi) are promising new chemotherapeutic agents currently in phase I and phase II clinical trials for the treatment of several types of human cancers (Martinet, 2011). Although the molecular mechanisms of action are not fully understood, compelling evidence indicates that HDACi induce aneuploidy by disrupting cell cycle checkpoints and inducing apoptosis with some specificity for cancer cells (Cimini *et al.*, 2003, Dowling *et al.*, 2005). However, a growing body of evidence indicates that different cell types exhibit distinct susceptibility to HDACi (Lee *et al.*, 2010, Ungerstedt *et al.*, 2005). Here, we set out to undertake a systematic analysis of the effects of low dose HDACi on female germ cell chromatin and chromosome stability in mammalian oocytes. Our results indicate that similar to cancer cells, mammalian germ cells exhibit an extreme susceptibility to TSA exposure at nanomolar concentrations. The potential mechanisms involved and the dynamics of chromosome condensation defects are discussed.

Results

Inhibition of histone deacetylases affects large-scale chromatin structure and induces dynamic euchromatin decondensation in pre-ovulatory oocytes

We have previously demonstrated that exposure of pre-ovulatory mouse oocytes to 100 nM TSA induces dramatic changes in large-scale chromatin structure (De La Fuente, 2006, De La Fuente *et al.*, 2004). Novel cancer therapeutic strategies advocate the use of low-dose drug treatments in an attempt to prevent acute cytotoxicity and exert specific anti-neoplastic effects through epigenetic reprogramming (Shen and Laird, 2012). Therefore, as an initial step to determine the mechanisms involved in the extreme susceptibility of the mammalian oocyte to HDACi we set out to analyze the dynamics of chromatin organization under high resolution and in real-time by live-cell imaging following exposure to a range of TSA concentrations. Germinal vesicle stage oocytes were cultured in medium containing the phosphodiesterase inhibitor milrinone to prevent germinal vesicle breakdown. Consistent with previous studies, the majority of pre-ovulatory oocytes recovered after gonadotropin stimulation exhibit a surrounded nucleolus (SN) configuration, which is associated with a more advanced stage of nuclear maturation and high developmental potential (Abe *et al.*, 2010, De La Fuente, 2006, De La Fuente and Eppig, 2001, De La Fuente *et al.*, 2004, Miyara, 2003, Wickramasinghe *et al.*, 1991, Zuccotti, 1995). Control SN oocytes exhibited the characteristic chromatin configuration in which heterochromatin domains are wrapped around the nucleolus and euchromatin fibers form a variable number of DNA clusters that are readily stained with histone H3 di-methylated at lysine 4, a histone modification associated with euchromatin regions (H3K4me₂; Fig. 1A). However, treatment with 15 to 33 nM TSA induced a striking decondensation of euchromatin fibers within 8 hours of treatment showing H3K4me₂ staining (green) that extended towards occupying the entire volume of the germinal vesicle in >90% ($p < 0.05$) of pre-ovulatory oocytes ($n = 735$). A representative image of the type of chromatin changes observed following exposure to 33 nM TSA is illustrated in (Fig. 1B). However, extensive chromatin decondensation was detected at all doses evaluated. These changes were associated with a state of global hyperacetylation of histone H4 at lysine 5 (H4K5ac; red) at all experimental doses tested as indicated by a specific immunoreactive band of 13 kDa (Fig. 2 A-B). These results reveal for the first time that chromatin configuration in pre-ovulatory oocytes is affected by nanomolar concentrations of TSA within hours of exposure, indicating an extreme susceptibility of the female gamete to HDACi treatment at sub-clinical doses.

To gain insight into the dynamics of chromatin decondensation induced by TSA exposure, live cell imaging experiments were conducted following microinjection of capped messenger RNA encoding GFP-labeled H2B protein (green). GV stage oocytes were maintained in medium containing milrinone to maintain meiotic arrest and were subjected to laser scanning confocal microscopy at 20 minutes intervals for 8 h in the absence (control) and presence of 100 nM TSA. Z-stack reconstructions were used to analyze the dynamics of changes in the degree of chromatin condensation and nuclear architecture. Control oocytes maintained a condensed chromatin configuration of the SN type throughout the entire 8 h imaging period. At times, significant movements of chromatin clusters that were not associated with the nucleolus

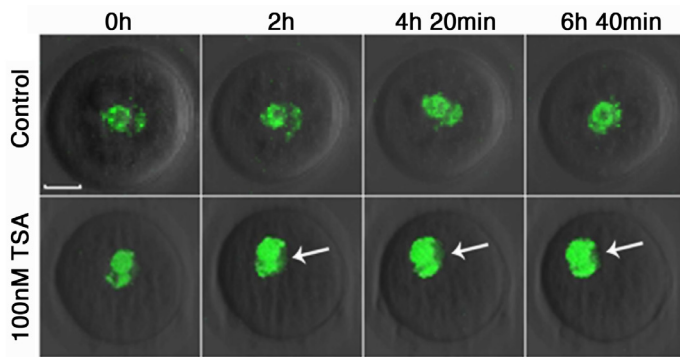


Fig. 3. Histone hyperacetylation interferes with large-scale chromatin remodeling in pre-ovulatory oocytes. Live cell imaging by laser-scanning confocal microscopy of control germinal vesicle (GV) stage oocytes (upper panel) and during exposure to 100 nM TSA (lower panel). Oocytes were microinjected with capped mRNA encoding a histone H2B-GFP fusion protein. Time-lapse Z-stack reconstructions were generated at 20 minutes intervals and clearly demonstrate rapid onset of chromatin decondensation within 2 h following TSA exposure (green) and loss of SN configuration in response to TSA treatment after 4 h (arrows). SN configuration and chromatin condensation remained unaltered in control oocytes.

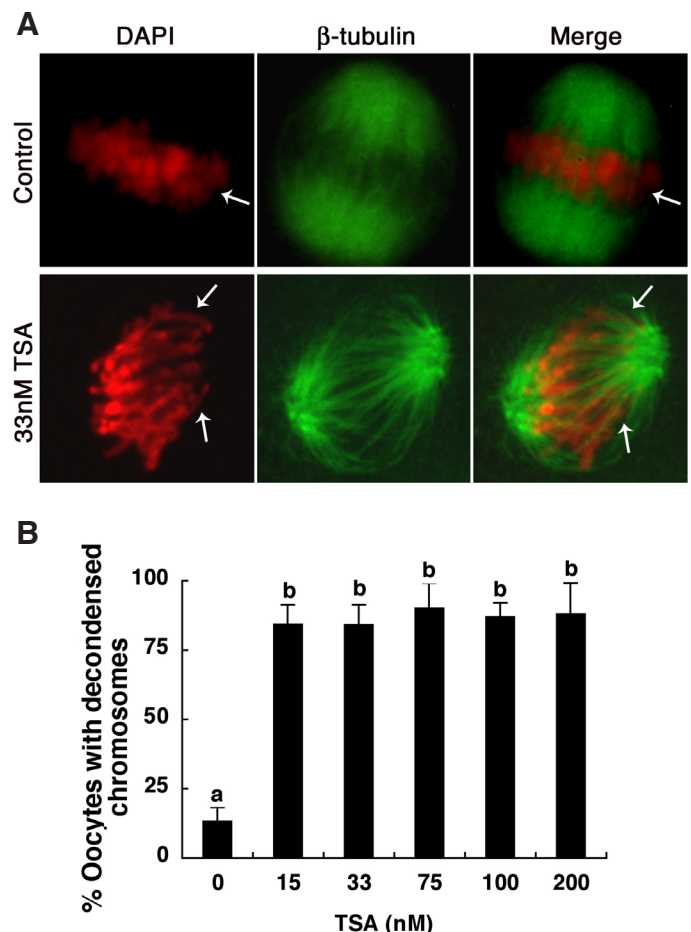
were detected, which provided the appearance of an intermediate chromatin configuration (Fig. 3, upper panel). However, a patent heterochromatin rim surrounding the nucleolus and condensed chromatin fibers were maintained at all time intervals evaluated. In contrast, treatment with 100 nM TSA led to a striking chromatin decondensation within 2 h of treatment (Fig. 3, lower panel, arrow), suggesting that HDACi lead to a rapid loss of the SN configuration and early onset chromatin decondensation. Dynamic changes in chromatin conformation revealed the appearance of decondensed chromatin fibers, which began to redistribute throughout the entire volume of the GV at 2 h and 4 h following TSA exposure, resulting in diffuse Histone H2B staining and loss of a discernible nucleolar configuration (Fig. 3). Collectively, our results demonstrate the presence of dynamic chromatin movements in the GV of control oocytes and notably, that doses as low as 15 nM of TSA were sufficient to induce changes in nuclear architecture leading to chromatin decondensation and histone hyperacetylation in the oocyte genome.

Low dose trichostatin A exposure predisposes mammalian oocytes to chromosome instability and aneuploidy

Exposure of mitotic cells to 33 nM TSA for 17 h induces only partial histone hyperacetylation and has no detectable effects

Fig. 4. Abnormal chromosome morphology in trichostatin A (TSA)-treated oocytes following *in vitro* maturation. (A) Control oocytes exhibit tightly condensed chromosomes (red, arrow) that were properly aligned at the equatorial plate following *in vitro* maturation for 16 h (upper panel). Severe chromosome decondensation (red, arrows) and abnormal chromosome morphology (arrows) was apparent in oocytes matured for 16 h in the presence of 33 nM TSA (lower panel). Spindle microtubules (green) were immunostained with a specific β -tubulin antibody. **(B)** TSA treatment during meiotic maturation significantly increases ($P < 0.05$) the proportion of oocytes with aberrant chromosome morphology at all concentrations tested (15 to 200 nM) compared to controls. Data are presented as the mean \pm SEM of at least three independent experimental replicates.

on chromosome segregation patterns (Sumer *et al.*, 2004). In contrast, we observed that a high proportion of pre-ovulatory oocytes exhibit disruptions in large-scale chromatin remodeling at the GV with doses as low as 15 nM TSA. Therefore, we determined the effects of TSA exposure at different concentrations on the patterns of chromosome segregation during *in vitro* oocyte maturation. Analysis of chromosome-microtubule interactions using laser scanning confocal microscopy revealed that in contrast with control oocytes that exhibit a barrel-shaped bipolar spindle (green) and metaphase chromosomes (red) tightly aligned at the equatorial region (Fig. 4A), exposure to TSA induced the formation of elongated chromosomes that appeared stretched at the early metaphase-anaphase transition (Fig. 4A; lower panel). Moreover, analysis of meiotic spindle configuration at different doses revealed that exposure to 15 nM TSA for 16 h was sufficient to induce a significant increase ($p < 0.05$) in the proportion (>80%) of maturing oocytes ($n = 352$) that exhibited elongated chromosomes, with similar effects observed at all doses evaluated (Fig. 4B). Moreover, exposure to TSA resulted in a dose dependent increase on the incidence of chromosome segregation defects ranging from (48%) at 15 nM TSA ($P < 0.05$) to (81%) at 100 nM TSA (Fig. 5A-B). Notably, a spectrum of chromosome segregation defects were observed including non-disjunction as well as lagging of single chromatids at spindle poles at the metaphase I-anaphase transition (Fig. 5A) with highly disorganized segregation of elongated chromatids at the metaphase II to anaphase II transition (Fig. 5A-B).



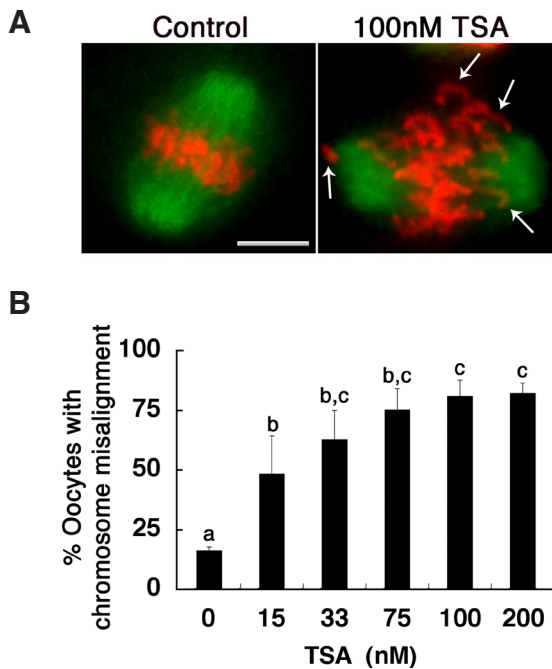


Fig. 5. Global histone hyperacetylation during meiosis induces chromosome lagging and non-disjunction (A) Meiotic spindle configuration following *in vitro* oocyte maturation in the absence or presence TSA for 16h. Control oocytes exhibit proper chromosome alignment (red) at the metaphase II spindle (green). In contrast, exposure to TSA induced a spectrum of chromosome segregation errors including single chromatid lagging and improper alignment of elongated chromatids. **(B)** Dose-response curve indicating a significant increase ($P < 0.05$) in the incidence of chromosome misalignment following TSA exposure. Chromosome segregation defects during oocyte maturation were observed with the lowest dose evaluated of 15 nM TSA. Data are presented as the mean \pm SEM of three independent experimental replicates. Different superscripts denote significant differences ($p < 0.05$). Scale bar, 10 μ M.

Effects of histone hyperacetylation on meiotic chromosome structure

To determine whether the chromosome elongation observed after TSA exposure results from a lack of proper chromosome condensation and chromatid individualization or as a consequence of the physical stretching of meiotic chromosomes during the metaphase to anaphase transition, we used live cell imaging to determine the behavior of meiotic chromosomes following disruption of large-scale chromatin structure. Consistent with our previous experiments, exposure to 100 nM TSA induced a detectable decondensation of euchromatin within 1–2 h after exposure of pre-ovulatory oocytes that exhibit the SN configuration (Fig. 6). Surprisingly, chromatid individualization takes place within 2 h following TSA exposure with bivalent chromosome formation clearly apparent by 2.5 h following germinal vesicle breakdown, although chromosomes do not condense to the same extent as controls. Chromosome congression into a metaphase I plate was observed by 8 h after which bivalents exhibit only restrictive movements (Fig. 6). Notably, TSA exposure seemed to induce a delayed onset into anaphase I until 13.5 h following germinal vesicle breakdown. At this stage, anaphase bridges were clearly observed resulting in a significant stretching of chromosomes during telophase and first polar body extrusion resulting in single chromatid lagging and a highly disorganized

metaphase II plate in which some chromatids were found tethered to the set of homologous chromosomes extruded into the first polar body (Fig. 6). Importantly, live cell imaging analysis of the few pre-ovulatory oocytes that retained the non-surrounded nucleolus (NSN) configuration revealed a significant delay in chromosome congression and the time of formation of a metaphase I plate until 14 h following germinal vesicle breakdown with persistence of a disorganized metaphase I configuration up to 18 h following germinal vesicle breakdown (Supplemental Fig. 1). These results indicate that TSA exposure interferes with proper sister chromatid segregation in oocytes with the SN configuration. In contrast, inhibition of histone deacetylases in oocytes that exhibit the NSN configuration interferes with meiotic progression and polar body extrusion even after 16 h of *in vitro* maturation.

The epigenetic mechanisms involved in abnormal chromosome structure following inhibition of HDACs are not known. Exposure to TSA during meiotic maturation induces a state of histone hyperacetylation in meiotic chromosomes (De La Fuente *et al.*, 2004, De La Fuente *et al.*, 2004, Kim *et al.*, 2003). Importantly, previous studies indicate that histone acetylation at lysine 16 (H4K16ac) might interfere with mono-methylation of histone H4 at lysine 20 (H4K20me), an important post-translational modification required for chromosome condensation in the pre-implantation embryo (Oda *et al.*, 2009, Rice, 2002). Therefore, we determined the interaction between H4K16ac and H4K20me in meiotic chromosomes as well as the type of epigenetic changes induced by TSA exposure at both centromeres and interstitial segments on meiotic chromosomes. Analysis of histone acetylation and histone methylation patterns under high-resolution confirmed the lack of histone acetylation marks in the chromosomes of control oocytes (Fig. 7). In contrast, exposure to TSA induced prominent chromosomal acetylation resulting in bright H4K5ac and H4K16ac signals at interstitial segments of elongated chromatids at the metaphase II stage. Notably, pericentric heterochromatin domains lacked H4K5Ac and H4K16ac staining and appeared clearly delineated as a DAPI bright domain containing two CREST signals (Fig. 7; Inset). Mono-methylation of histone H4 at lysine 20 (H4K20me) was detected in both, interstitial regions as well as pericentric heterochromatin in the chromosomes of control oocytes with no prominent differences observed after TSA exposure. These results indicate that inhibition of histone deacetylases during meiosis induces distinct changes in epigenetic modifications at interstitial chromosomal regions and pericentric heterochromatin domains and that, in contrast with somatic cells the presence of H4K16ac in meiotic chromosomes does not interfere with H4K20me. Importantly, these results also indicate that the changes in chromosome condensation induced by TSA exposure are not due to lack of H4K20me.

Inhibition of histone deacetylases induces a redistribution of structural proteins associated with chromosome condensation

In mammalian cells, the condensin protein complex is required for chromosome condensation during mitosis (Losada and Hirano, 2005). Importantly, the structural maintenance of chromosome 4 (SMC4) protein is essential for the control of large-scale chromosome assembly and segregation (Coelho *et al.*, 2003). In addition, histone H3 phosphorylation at lysine 10 has been associated with chromosome condensation (Hendzel *et al.*, 1997). Therefore, we determined the effect of TSA exposure on these critical factors required for chromosome segregation. Analysis of chromosome

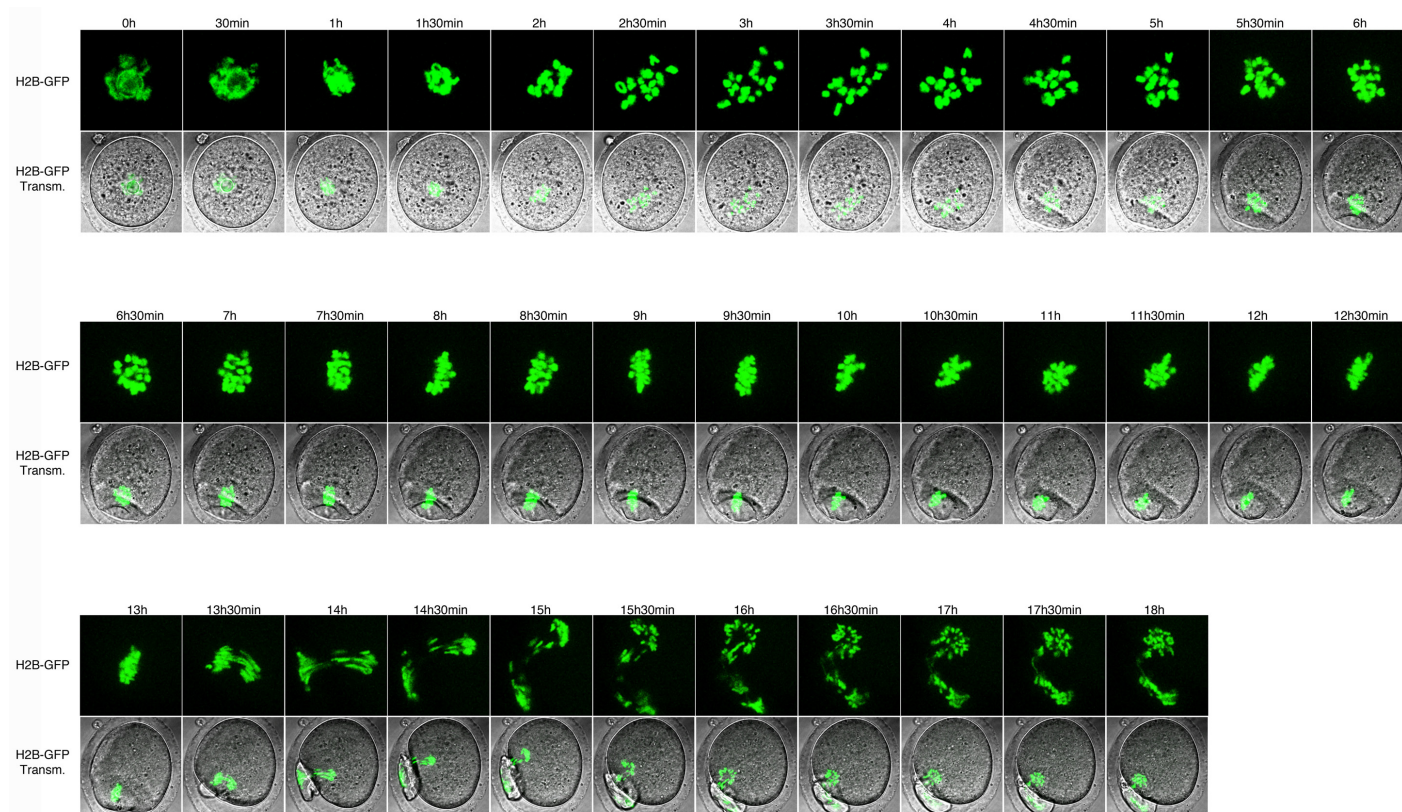


Fig. 6. Global histone hyperacetylation during meiosis interferes with sister chromatid separation. Time-lapse analysis of chromosome segregation patterns in the presence of 100 nM TSA. Oocytes were microinjected with capped mRNA encoding a histone H2B-GFP fusion protein. Time-lapse Z-stack reconstructions were generated at 30 minutes intervals over an 18 h period. Histone hyperacetylation following TSA exposure induces decondensation of chromatin fibers. Notably, bivalent chromosome formation is completed by 2 h after germinal vesicle breakdown (GVBD). Chromosome congression is complete by 8 h after GVBD. However, the onset of anaphase is delayed until 14 h after GVBD. Prominent anaphase bridges can be detected and result in the formation of axial chromatid elongation and abnormal chromosome morphology.

localization patterns under high resolution indicate that in control oocytes, histone H3 phosphorylation at serine 10 (H3S10ph; red) is a prominent mark of interstitial regions of meiotic chromosomes where it is found in a diffuse pattern throughout the entire chromatid length at the metaphase I and metaphase II stage (Fig. 8 A-B). In contrast, the condensin protein SMC4 (green) is exclusively found at the central chromatid axis of both metaphase I and metaphase II stage chromosomes. Notably, exposure to TSA induced both a partial reduction on H3S10ph signals at interstitial chromosome segments as well as a prominent accumulation of this epigenetic mark at pericentric heterochromatin on metaphase I and metaphase II stage chromosomes (Fig. 8 A-B). Moreover, while TSA exposure reduced the association of SMC4 protein with pericentric heterochromatin domains, no major differences were detected on the immunoreactivity of SMC4 at the central chromatid axis (Fig. 8 A-B; Insets). These results indicate that inhibition of histone deacetylases interferes with the pericentric heterochromatin localization of critical chromatin modifications and structural proteins required for accurate chromosome condensation and sister chromatid segregation.

Discussion

Proper chromosome condensation as well as the timely resolution of sister chromatid cohesion are essential for the accurate

segregation of chromosomes during both mitotic and meiotic cell division (Nasmyth, 2002, Petronczki *et al.*, 2003, Yu and Koshland, 2005). We and others have previously demonstrated that inhibition of histone deacetylases following exposure of maturing oocytes to TSA induces dramatic changes in large-scale chromatin structure and abnormal chromosome segregation (De La Fuente *et al.*, 2006, De La Fuente *et al.*, 2004, Kim *et al.*, 2003). However, the epigenetic mechanisms involved in this process remained to be determined. Here, we provide evidence indicating that the mammalian oocyte is extremely susceptible to histone deacetylase inhibitors. Our results indicate that histone hyperacetylation induces dramatic changes in large-scale chromatin structure within hours following TSA exposure and results in a spectrum of chromosome segregation defects in a dose dependent manner. Live cell imaging studies indicate that global histone hyperacetylation is associated with extensive euchromatin decondensation. Notably, bivalent chromosome formation ensues, resulting in the formation of elongated chromatids that exhibit extensive histone H4 acetylation at interstitial segments. In contrast, pericentric heterochromatin domains accumulate histone H3 phosphorylation. Finally, we show that alterations in chromosome structure as well as the degree of chromosome decondensation observed following TSA exposure are not due to lack of condensin protein SMC4 suggesting that chromosome elongation at anaphase is due to interference with proper sister chromatid separation as indicated by the presence

of anaphase bridges in hyperacetylated chromosomes.

Previous studies conducted in human somatic (HeLa) cell lines suggest that in addition to epigenetic changes and histone modifications, HDACi also induce a striking reorganization of large-scale chromatin structure. For example, exposure of HeLa cells to 200 nM TSA for 48 hours has been shown to induce decondensation of interphase nuclei and a consequent increase in 56% in nuclear volume in human somatic cells (Bartova *et al.*, 2005, Toth *et al.*, 2004). The mechanisms involved in this process are not fully understood. However, fluorescence recovery after photo bleaching (FRAP) analysis indicates that in somatic cells, TSA increases the mobility and phosphorylation status of core linker histones (H1.5) and induces an up-regulation of linker histone H1 transcript expression in addition to global changes in histone deacetylation (Rao *et al.*, 2007). Several lines of evidence now indicate that different mechanisms seem to be activated in mammalian oocytes following TSA exposure. First, a dose as low as 15 nM TSA for 8 hours proved sufficient to induce a dramatic decondensation in the majority of mouse oocyte nuclei at the GV stage. Second, chromatin decondensation in the GV takes place in the absence of any changes in the levels of expression or electrophoretic mobility of the oocyte specific linker histone H1FOO (De La Fuente *et al.*, 2004). The effects of TSA on large-scale chromatin structure vary according to the cell type and stage of the cell cycle with pro-metaphase cells exhibiting the highest sensitivity to TSA exposure (Bartova *et al.*, 2005, Toth *et al.*, 2004). Therefore, we propose that by virtue of their protracted arrest at the G2/M transition, mammalian oocytes exhibit an extreme susceptibility to TSA exposure. However, further studies will be required to determine whether TSA induces changes in the binding affinity and/or mobility of Histone H1FOO or additional linker histones in the mammalian oocyte genome.

Global histone hyperacetylation may recruit remodeling complexes that change the higher order conformation of chromatin fibers (Bartova *et al.*, 2005). However, this mechanism may also differ in the oocyte genome. For example, in HeLa cells, inhibition of HDACs resulted in a global increase in H3K9/H3K4 methylation and H3K9 acetylation as detected by western blot analysis. In addition, the intensity of H3K4me increased in the somatic cell nucleus after treatment with TSA (Dowling *et al.*, 2005). In contrast, the levels of this histone posttranslational modification remain unchanged in pre-ovulatory oocytes exposed to TSA. Therefore, our results are consistent with the presence of a unique epigenetic control of chromatin remodeling in the mammalian oocyte.

In spite of the extensive decondensation of chromatin fibers observed following TSA exposure, formation of meiotic chromosome bivalents ensues, albeit with impaired axial chromatid condensation and associated with abnormal chromosome segregation in a high proportion of oocytes. Notably, in contrast with somatic cells in which exposure to 33 nM TSA failed to induce abnormal mitotic chromosome segregation, a high proportion of pre-ovulatory oocytes exhibit chromosome and chromatid lagging as well as chromosome non-disjunction after a low dose (15 nM) TSA exposure. In contrast, lagging chromosomes were observed in only 2% of cells following exposure of human lung fibroblasts and HeLa cells to 500 ng/ml TSA for 7 h (Cimini *et al.*, 2003). These results underscore the extreme susceptibility of the mammalian oocyte to HDACi. The spectrum of chromosome segregation defects observed indicates that histone hyperacetylation during oocyte meiotic maturation interferes with accurate chromosome segregation through several

mechanisms. For example, the presence of chromosome non-disjunction is consistent with abnormal centromere function and the establishment of monopolar microtubule attachments (Compton, 2011, Gregan *et al.*, 2011), while the presence of chromatid lagging indicate abnormal sister chromatid segregation and the formation of abnormal 'merotelic' chromosome-microtubule attachments (Compton, 2011, Gregan *et al.*, 2011).

Exposure of somatic cells to TSA induces dramatic changes in the nuclear localization of centromeric domains and interferes with the binding of heterochromatin protein 1 (HP1) to pericentric heterochromatin after two or three cell cycles (Taddei *et al.*, 2001, Taddei *et al.*, 2005). Importantly, histone hyperacetylation during meiosis interferes with the recruitment of the chromatin remodeling protein ATRX to pericentric heterochromatin within a short period (14 hours) of *in vitro* oocyte maturation (De La Fuente *et al.*, 2004)

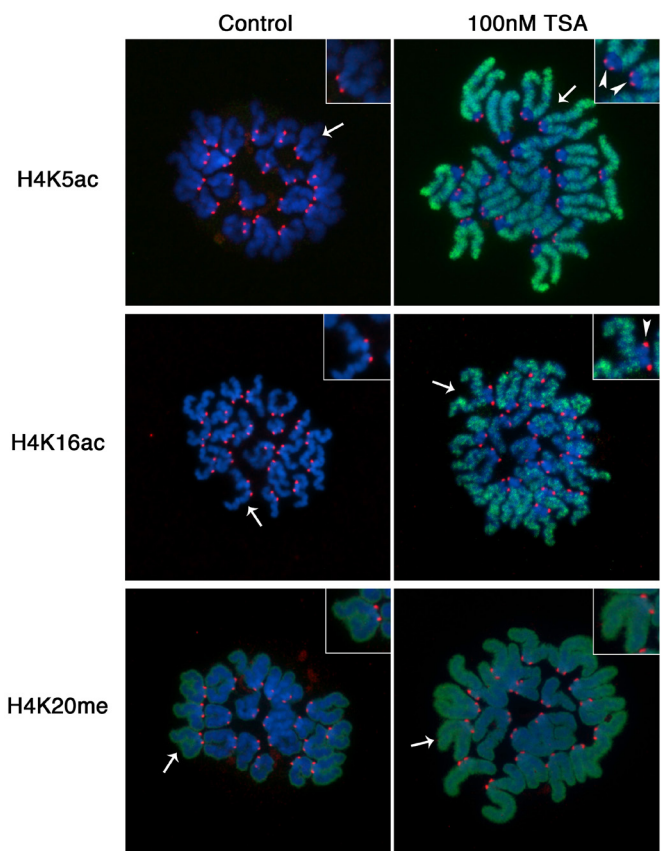


Fig. 7. Differential effects of a short trichostatin A (TSA) exposure on interstitial and pericentric heterochromatin domains of meiotic chromosomes. Control oocytes matured in the absence of TSA demonstrated normal chromosome morphology (blue) and global histone deacetylation (lack of H4K5ac signals) as determined by high-resolution cytogenetic analysis (upper panel). Treatment with 100 nM TSA during *in vitro* maturation induced chromatin decondensation and hyperacetylation of lysine 5 in histone H4 at interstitial chromosome segments (green), but not pericentric heterochromatin domains (insets). Acetylation of histone H4 at lysine 16 (H4K16; green) is also restricted to chromosome interstitial segments and remains excluded from pericentric heterochromatin domains (inset). The position of the centromere is indicated by CREST signals (red). Note the absence of histone acetylation at centromeric domains (mid panel). Control and TSA treated oocytes exhibit similar levels of mono-methylation of histone H4 at lysine 20 (H4K20me).

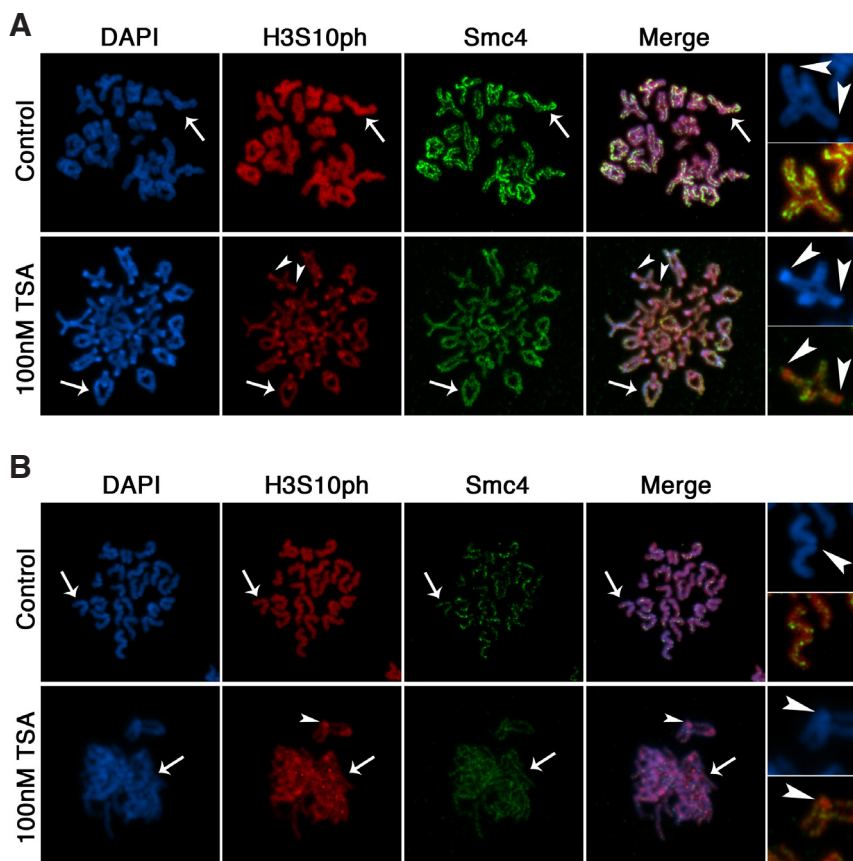


Fig. 8. Localization of the condensing protein SMC4 to the central chromatid axis of hyperacetylated chromosomes. (A) Localization of epigenetic markers associated with chromosome condensation in the presence or absence of 100 nM TSA in maturing oocytes at the metaphase I stage. Histone H3 phosphorylation at serine 10 (H3S10ph; red) exhibits a diffuse localization throughout the entire length of properly condensed bivalents at the metaphase I stage. In contrast, the condensin protein SMC4 (green) is exclusively localized to the central chromatid axis (insets) including centromeric domains (arrows). Treatment with TSA induced chromosome elongation and a redistribution of H3S10ph at centromeric domains resulting in increased levels of histone H3 phosphorylation at pericentric heterochromatin (arrow head, lower panel) compared to controls. (B) High resolution chromosome analysis at the metaphase II stage. Histone hyperacetylation induces a modest reduction in the levels of interstitial chromosome H3S10ph staining and a redistribution of this epigenetic mark to pericentric heterochromatin (inset; arrow). Although hyperacetylated chromosomes exhibit axial chromatid elongation, the condensin protein SMC4 is still detectable at the central chromatid axis.

while inducing an accumulation of histone H3 phosphorylation at centromeric domains of elongated chromosomes (this study), suggesting that HDACi affect critical pathways required for the epigenetic control of centromere function. Therefore, our results indicate that abnormal centromere-microtubule interactions following TSA exposure contribute to the high incidence of chromosome segregation defects.

The presence of single chromatid lagging suggests that histone hyperacetylation during meiosis interferes with proper sister chromatid segregation. Notably, in human somatic cells TSA induced abnormal chromosome condensation and persistent cohesion along sister chromatids resulting in the formation of lagging chromosomes with single or paired sister chromatids (Cimini *et al.*, 2003). Consistent with these observations, live cell imaging

analysis of oocyte maturation revealed that TSA induced a significant delay in anaphase I onset and results in the formation of anaphase chromatin bridges providing evidence for the persistence of sister chromatid cohesion in maturing oocytes with hyperacetylated chromosomes. Our results indicate that histone hyperacetylation prevents proper chromosome condensation during oocyte meiotic maturation. The functional interaction between histone modifications, chromosome condensation and sister chromatid cohesion during meiosis are not clear at present. Monomethylation of histone H4 at lysine 20 (H4K20me) is essential for proper chromosome condensation in the mammalian oocyte and pre-implantation embryo (Oda *et al.*, 2009). Notably, previous studies indicate that hyperacetylation of histone H4 at lysine 16 (H4K16ac) antagonizes the establishment of H4K20me marks on mitotic chromosomes (Oda *et al.*, 2009; Rice, 2002). However, although TSA exposure induced a striking hyperacetylation of H4K16ac at interstitial chromosomal segments, no changes were observed on the levels or chromosomal localization of H4K20me on meiotic chromosomes indicating that lack of proper chromosome condensation in response to TSA exposure is induced by mechanisms other than loss of H4K20me in the maturing oocyte. In contrast, our results indicate a slight reduction of histone H3 phosphorylation (H3S10ph) at interstitial segments of meiotic chromosomes and a prominent accumulation of this chromatin mark at pericentric heterochromatin. Phosphorylation of histone H3 at Ser10 is an essential epigenetic mark that is initially established at pericentric heterochromatin and its subsequent spreading through interstitial chromosome segments has been correlated with mitotic chromosome condensation (Hendzel *et al.*, 1997). Together with the loss of condensin protein SMC4 from pericentric heterochromatin, our results indicate that TSA exposure disrupts critical structural components of the meiotic centromere.

Although not formally demonstrated, previous studies suggested that reduction of H3S10ph at hyperacetylated chromosomes during mitosis might prevent binding of condensation factors such as Topoisomerase II and/or component molecules of the condensin complex (Cimini *et al.*, 2003). The Condensin I complex (SMC2 and SMC4) and its distinct regulatory subunits of the Condensin complex II are essential for chromosome individualization in the mammalian oocyte (Lee *et al.*, 2011). Moreover, SMC4 is required for sister chromatid separation during mitosis in *Drosophila* cells where lack of proper chromosome condensation after loss of SMC4 function interferes with sister chromatid cohesion (Coelho *et al.*, 2003). Remarkably, our results indicate that bivalent meiotic chromosome formation takes place in the presence of histone hyperacetylation and highly decondensed chromatin and that SMC4 is only displaced from pericentric heterochromatin regions, while SMC4 remains detectable at the axial chromatid cores of meiotic chromosomes at the metaphase I and metaphase II stage. These

results indicate that, chromosome elongation following TSA exposure may arise as a consequence of the physical stretching induced by anaphase bridge formation most likely due to abnormal sister chromatid separation. In support of this hypothesis, FLIM-FRET analysis indicates that maximum chromatin compaction during mitosis takes place during late anaphase (Lleres *et al.*, 2009). Thus, abnormal sister chromatid separation may interfere with this process resulting in elongation of meiotic chromosomes following TSA exposure. Studies are in progress to determine whether histone acetylation status may affect chromosome arm cohesion and axial chromatid structure by interfering with DNA decatenation of sister chromatids during oocyte meiotic maturation.

Materials and Methods

Oocyte collection, culture and treatment

Fully-grown oocytes at the germinal vesicle (GV) stage were obtained as cumulus-oocyte-complexes (COCs) from 22-day old (C57BL/6J × DBA/2J) F1 mice 48 h following administration of 5 I.U. pregnant mare's serum gonadotropin i.p. (PMSG; EMD Biosciences, La Jolla, CA) as described previously (De La Fuente *et al.*, 2004). Briefly, COCs were collected in 3 ml Minimal Essential Medium (MEM) supplemented with 3 mg/ml BSA (Sigma, St. Louis, MO) and 10 μM Milrinone (Sigma) to inhibit GV breakdown (GVBD). Surrounding cumulus cells were gradually removed by repeated pipetting and denuded oocytes were transferred to fresh medium before allocation to different experimental groups. Oocytes were cultured for 8 hours at 37 °C under an atmosphere of 5% O₂, 5% CO₂ and 90% N₂ in the presence of the histone deacetylase inhibitor Trichostatin A (TSA, Biomol, Research Lab Inc., Plymouth Meeting, PA) at concentrations of 0 to 200 nM as indicated. For *in vitro* maturation experiments, oocytes were released from Milrinone block and transferred to fresh medium supplemented with TSA for a period of 16 hours.

Western blot analysis

TSA treated and untreated (control) GV stage oocytes were washed in PBS supplemented with protease inhibitors (10 μg/ml leupeptin, pepstatin and aprotinin, 1 mM DTT and 1 mM pefabloc; Sigma) and resuspended in 1 ml of ice-cold lysis buffer (10 mM Tris-HCl, 50 mM sodium bisulfite, 1% Triton X-100, 10 mM MgCl₂, 8.6% sucrose, pH 6.5) and freeze-thawed 10 times in liquid nitrogen. Oocyte nuclei were collected by centrifugation at 1100g for 10 min, washed three times in lysis buffer, followed by a single wash in TE buffer (10 mM Tris-HCl, 13 mM EDTA, pH 7.4). The pellet was then re-suspended in 15 μl of ice-cold autoclaved H₂O using a vortex mixer; sulfuric acid was added to a final concentration of 0.2N. The samples were incubated overnight at 4 °C before centrifugation for 5 min at 13,000 rpm. The acid-soluble histone fraction in the supernatant was then transferred to a new vial before supplementing 5 μl of Laemmli buffer (Biorad, Hercules, CA) supplemented with 0.71 M β-Mercaptoethanol (Biorad) and storage at -80 °C. For SDS-PAGE, samples were thawed and heated to 100 °C for 8 min. Proteins were separated by electrophoresis in a 4% stacking gel and a 12% polyacrylamide separating gel containing 0.1% SDS and transferred onto a hydrophobic polyvinylidene difluoride (PVDF) membrane (Amersham, Piscataway, NJ) for 90 min at 100 V. The membrane was washed twice in TBS buffer (pH 7.4; Biorad) containing 0.1% Tween 20 (TBST) and then blocked in TBST containing 5% non-fat dry milk for 1 h at room temperature. Immunodetection of the acetylated histone H4 protein was conducted using a rabbit anti-pan-Ac-histone H4 antibody (1:1000; Upstate Biotechnology) at 4 °C overnight followed by exposure to a HRP-conjugated anti-rabbit secondary antibody (1:5000; Jackson ImmunoResearch, West Grove, PA). Immunodetection of beta-tubulin was conducted to serve as loading control.

Immunocytochemistry of whole mount oocytes and chromosomal spreads

Sub-cellular protein localization was assessed in whole mount oocytes

at the GV stage. Oocytes were fixed following 16 h of *in vitro* maturation with 4% paraformaldehyde supplemented with 1% Triton X for 10 min at room temperature followed by a subsequent blocking step in 10% fetal calf serum in PBS and 0.2% Tween 20 (PBT) overnight. Whole mount oocytes were immuno-stained using a polyclonal rabbit anti-histone H4 acetylated at lysine 5 (H4K5ac) antibody (1:1000, Millipore, Billerica, MA) and a mouse anti-β-tubulin antibody (1:500, Sigma). In addition, GV stage oocytes were also immunolabeled with a polyclonal rabbit anti-histone H3 dimethylated at lysine 4 (H3K4me₂) antibody (1:400, Millipore). The secondary antibodies, Alexa-fluor 488 goat anti-rabbit IgG, Alexa-fluor 555 goat anti-rabbit IgG and Alexa-fluor 488 goat anti-mouse IgG were purchased from Molecular Probes, Inc (Eugene, OR) and used at a 1:500 dilution. Slides were mounted using 8 μl of mounting medium supplemented with DAPI (Vectashield; Vector Laboratories, Burlingame, CA), to counterstain chromatin. Oocytes were examined on a DMRE microscope equipped with epifluorescence (Leica Microsystems) using a 100x objective as described (De La Fuente *et al.*, 2004).

To conduct high-resolution cytogenetic analyses, chromosomal spreads were prepared from zona-free oocytes at different stages of meiotic maturation (Yang *et al.*, 2009). The zona pellucida was removed with 3 mg/ml pronase (Sigma) in PBS. Zona-free oocytes were rinsed twice in MEM medium and immediately processed for cytogenetic preparations. Chromosomal proteins were cross-linked by spreading the oocytes on wet glass slides containing 1% paraformaldehyde and 0.15% Triton X 100. Slides were allowed to dry at room temperature and stored at -20 °C until further use. Chromosomal spreads were immunostained with a rabbit anti-H4K5ac antibody (1:1000), a mouse anti-histone H3 phosphorylated at serine 10 (H3S10ph) (1:1000), a rabbit anti-H4K16ac antibody (1:1000; Millipore), or H4K20me (1:1000; Abcam) or an anti-SMC4 antibody (1:1000; Bethyl Laboratories) prior to counterstaining with DAPI.

Live cell imaging

To visualize chromatin dynamics as well as chromosome segregation patterns in response to TSA treatment, time-lapse image acquisition was performed following microinjection of capped messenger RNA encoding a histone H2B-Green fluorescence (H2B-GFP) fusion protein into the cytoplasm of fully-grown GV stage oocytes to visualize chromatin in live oocytes as described (Baumann *et al.*, 2010). Capped messenger RNA was *in vitro* transcribed using a modified pIVT vector containing a pBOS-H2BGFP-derived coding sequence of a H2B-GFP fusion protein containing 5' and 3' *Xenopus* globin UTR's (a kind gift of Dr. R. Schultz). A total of 1 μg of linearized pIVT-H2BGFP plasmid was *in vitro* transcribed using the mMessage mMachine Kit (Ambion) according to manufacturers recommendations. Microinjected oocytes were cultured in the presence of 10 μM milrinone for 3-4 h to prevent germinal vesicle breakdown and allow for recombinant protein expression. Oocytes were matured *in vitro* in a 50 μl drop of MEM medium on a TOKAI-HIT environmental chamber (Nikon) maintained at 37 °C under an atmosphere of 5% O₂, 5% CO₂ and 90% N₂ under conditions and laser excitation parameters compatible with normal meiotic progression. Specifically, chromatin organization and chromosome segregation patterns in response to TSA (100 nM) treatment were monitored by 3D time-lapse microscopy at 20 minutes intervals for 8 h and at 30 minute intervals for 16 h at 37 °C on a Leica TCS-SP5 laser scanning confocal microscope equipped with a 10x objective lens and 3.1x digital zoom following excitation of GFP protein with a 488 nm argon laser and detected using a 505-550 nm emission filter. Live cell imaging data were analyzed by 3D reconstructions using LAS AF software (Leica, Bannockburn, IL).

Statistical analysis

Data are presented as the mean percentage of at least three independent experiments; variation among replicates is presented as the standard error of the mean (SEM). The percentage of oocytes at different stages of meiotic maturation and the percentage of GV stage oocytes with decondensed chromatin morphology in the presence or absence of TSA were analyzed

by using arcsine transformed data and compared by one-way analysis of variance (ANOVA) as well as following the comparison of all pairs by Tukey–Kramer HSD using JMP Start Statistics (SAS Institute, Inc., Cary, NC). Differences were considered significant when $p < 0.05$.

Acknowledgements

This research was supported by grants from the National Institute of Child Health and Human Development (NICHD), National Institutes of Health (2RO1-HDO42740) and the Georgia Cancer Coalition to R. De La Fuente. Research in M.M. Viveiros laboratory is supported by grant (HD071330) from the NIH.

References

- ABE, K.I., INOUE, A., SUZUKI, M.G. and AOKI, F. (2010). Global Gene Silencing is caused by the Dissociation of RNA Polymerase II from DNA in Mouse Oocytes. *J. Reprod. Dev.* 56: 502-507.
- ADENOT, P.G., MERCIER, Y., RENARD, J.P. and THOMPSON, E.M. (1997). Differential H4 acetylation of paternal and maternal chromatin precedes DNA replication and differential transcriptional activity in pronuclei of 1-cell mouse embryos. *Development* 124: 4615-25.
- AKIYAMA, T., NAGATA, M. and AOKI, F. (2006). Inadequate histone deacetylation during oocyte meiosis causes aneuploidy and embryo death in mice. *Proc Natl Acad Sci USA* 103: 7339-44.
- BARTOVA, E., PACHERNIK, J., HARNICAROVA, A., KOVARIK, A., KOVARIKOVA, M., HOFMANOVA, J., SKALNIKOVA, M., KOZUBEK, M. and KOZUBEK, S. (2005). Nuclear levels and patterns of histone H3 modification and HP1 proteins after inhibition of histone deacetylases. *J Cell Sci* 118: 5035-46.
- BAUMANN, C., VIVEIROS, M.M. and DE LA FUENTE, R. (2010). Loss of Maternal ATRX Results in Centromere Instability and Aneuploidy in the Mammalian Oocyte and Pre-Implantation Embryo. *PLoS Genet* 6: e1001137.
- CIMINI, D., MATTIUZZO, M., TOROSANTUCCI, L. and DEGRASSI, F. (2003). Histone hyperacetylation in mitosis prevents sister chromatid separation and produces chromosome segregation defects. *Mol Biol Cell* 14: 3821-33.
- COELHO, P.A., QUEIROZ-MACHADO, J. and SUNKEL, C.E. (2003). Condensin-dependent localisation of topoisomerase II to an axial chromosomal structure is required for sister chromatid resolution during mitosis. *J. Cell Sci.* 116: 4763-4776.
- COMPTON, D.A. (2011). Mechanisms of aneuploidy. *Curr. Opin. Cell Biol.* 23: 109-113.
- DE LA FUENTE, R. (2006). Chromatin modifications in the germinal vesicle (GV) of mammalian oocytes. *Dev Biol* 292: 1-12.
- DE LA FUENTE, R., BAUMANN, C., FAN, T., SCHMIDTMANN, A., DOBRINSKI, I. and MUEGGEL, K. (2006). Lsh is required for meiotic chromosome synapsis and retrotransposon silencing in female germ cells. *Nat Cell Biol* 8: 1448-54.
- DE LA FUENTE, R., BAUMANN, C. and VIVEIROS, M. (2012). Chromatin Structure and ATRX Function in Mouse Oocytes. *Results Probl Cell Differ.* 55: 45-68.
- DE LA FUENTE, R. and EPPIG, J.J. (2001). Transcriptional activity of the mouse oocyte genome: Companion granulosa cells modulate transcription and chromatin remodeling. *Dev. Biol.* 229: 224-236.
- DE LA FUENTE, R., VIVEIROS, M., WIGGLESWORTH, K. and EPPIG, J. (2004). ATRX, a member of the SNF2 family of helicase /ATPases, is required for chromosome alignment and meiotic spindle organization in metaphase II stage mouse oocytes. *Dev. Biol.* 272: 1-14.
- DE LA FUENTE R., VIVEIROS, M., BURNS, K., ADASHI, E., MATZUK, M. and EPPIG, J. (2004). Major chromatin remodeling in the germinal vesicle (GV) of mammalian oocytes is dispensable for global transcriptional silencing but required for centromeric heterochromatin function. *Dev Biol.* 275: 447-58.
- DOWLING, M., VOONG, K.R., KIM, M., KEUTMANN, M.K., HARRIS, E. and KAO, G.D. (2005). Mitotic spindle checkpoint inactivation by trichostatin defines a mechanism for increasing cancer cell killing by microtubule-disrupting agents. *Cancer Biol Ther* 4: 197-206.
- GREGAN, J., POLAKOVA, S., ZHANG, L., TOLIC-NORRELYKKE, I.M. and CIMINI, D. (2011). Merotelic kinetochore attachment: causes and effects. *Trends Cell Biol.* 21: 374-381.
- HENDZEL, M.J., WEI, Y., MANCINI, M.A., VAN HOOSER, A., RANALLI, T., BRINKLEY, B.R., BAZETT-JONES, D.P. and ALLIS, C.D. (1997). Mitosis-specific phosphorylation of histone H3 initiates primarily within pericentromeric heterochromatin during G2 and spreads in an ordered fashion coincident with mitotic chromosome condensation. *Chromosoma* 106: 348-360.
- KAGEYAMA, S.-I., LIU, H., KANEKO, N., OOGA, M., NAGATA, M. and AOKI, F. (2007). Alterations in epigenetic modifications during oocyte growth in mice. *Reproduction* 133: 85-94.
- KIM, J., LIU, H., TAZAKI, M., NAGATA, M. and AOKI, F. (2003). Changes in histone acetylation during mouse oocyte meiosis. *J Cell Biol.* 162: 37-46.
- KIMMINS, S. and SASSONE-CORSI, P. (2005). Chromatin remodelling and epigenetic features of germ cells. *Nature* 434: 583-9.
- KOTA, S.K. and FEIL, R. (2010). Epigenetic Transitions in Germ Cell Development and Meiosis. *Dev. Cell* 19: 675-686.
- LEE, J., OGUSHI, S., SAITOU, M. and HIRANO, T. (2011). Condensins I and II are essential for construction of bivalent chromosomes in mouse oocytes. *Molec. Biol. Cell* 22: 3465-3477.
- LEE, J.H., CHOY, M.L., NGO, L., FOSTER, S.S. and MARKS, P.A. (2010). Histone deacetylase inhibitor induces DNA damage, which normal but not transformed cells can repair. *Proc. Natl. Acad. Sci. USA* 107: 14639-14644.
- LI, E. (2002). Chromatin modification and epigenetic reprogramming in mammalian development. *Nat Rev Genet* 3: 662-73.
- LLERES, D., JAMES, J., SWIFT, S., NORMAN, D.G. and LAMOND, A.I. (2009). Quantitative analysis of chromatin compaction in living cells using FLIM-FRET. *J. Cell Biol.* 187: 481-496.
- LOSADA, A. and HIRANO, T. (2005). Dynamic molecular linkers of the genome: the first decade of SMC proteins. *Genes Dev* 19: 1269-87.
- MA, P., PAN, H., MONTGOMERY, R.L., OLSON, E.N. and SCHULTZ, R.M. (2012). Compensatory functions of histone deacetylase 1 (HDAC1) and HDAC2 regulate transcription and apoptosis during mouse oocyte development. *Proc. Natl. Acad. Sci. USA* 109: E481-E489.
- MARTINET N, B.P. (2011). Interpreting clinical assays for histone deacetylase inhibitors. *Cancer Manag Res* 3: 117-41.
- MIYARA F, M.C., DUMONT-HASSAN M, MEUR AL, COHEN-BACRIE P, AUBRIOT FX, GLISSANT A, NATHAN C, DOUARD S, STANOVICI A, DEBEY P. (2003). Chromatin configuration and transcriptional control in human and mouse oocytes. *Mol Reprod Dev.* 64: 458-70.
- NASMYTH, K. (2002). Segregating sister genomes: the molecular biology of chromosome separation. *Science* 297: 559-65.
- ODA, H., OKAMOTO, I., MURPHY, N., CHU, J., PRICE, S.M., SHEN, M.M., TORRESPADILLA, M.E., HEARD, E. and REINBERG, D. (2009). Monomethylation of Histone H4-Lysine 20 Is Involved in Chromosome Structure and Stability and Is Essential for Mouse Development. *Molec. Cell Biol.* 29: 2278-2295.
- PATTERTON, D. and WOLFFE, A.P. (1996). Developmental roles for chromatin and chromosomal structure. *Dev Biol* 173: 2-13.
- PETRONCZKI, M., SIOMOS, M. and NASMYTH, K. (2003). Un menage a quatre: the molecular biology of chromosome segregation in meiosis. *Cell* 112: 423-40
- RAO, J., BHATTACHARYA, D., BANERJEE, B., SARIN, A. and SHIVASHANKAR, G.V. (2007). Trichostatin-A induces differential changes in histone protein dynamics and expression in HeLa cells. *Biochem. Biophys. Res. Commun.* 363: 263-268.
- REVENKOVA, E., EIJPE, M., HEYTING, C., GROSS, B. and JESSBERGER, R. (2001). Novel meiosis-specific isoform of mammalian SMC1. *Molec. Cell Biol.* 21: 6984-6998.
- REVENKOVA, E., EIJPE, M., HEYTING, C., HODGES, C., HUNT, P., LIEBE, B., SCHERTHAN, H. and JESSBERGER, R. (2004). Cohesin SMC1 beta is required for meiotic chromosome dynamics, sister chromatid cohesion and DNA recombination. *Nat Cell Biol.* 6: 555-62.
- RICE, J.C., NISHIOKAK, SARMAK, STEWARD R, REINBERG D, ALLIS CD. (2002). Mitotic-specific methylation of histone H4 Lys 20 follows increased PR-Set7 expression and its localization to mitotic chromosomes. *Genes Dev* 16: 2225-30.
- SARMENTO, O.F., DIGILIO, L.C., WANG, Y., PERLIN, J., HERR, J.C., ALLIS, C.D. and COONROD, S.A. (2004). Dynamic alterations of specific histone modifications during early murine development. *J Cell Sci* 117: 4449-59.
- SHEN, H. and LAIRD, P.W. (2012). In Epigenetic Therapy, Less Is More. *Cell Stem Cell* 10: 353-354.
- SUMER, H., SAFFERY, R., WONG, N., CRAIG, J.M. and CHOO, K.H. (2004). Effects of scaffold/matrix alteration on centromeric function and gene expression.

- J Biol Chem* 279: 37631-9.
- TADDEI, A., MAISON, C., ROCHE, D. and ALMOUZNI, G. (2001). Reversible disruption of pericentric heterochromatin and centromere function by inhibiting deacetylases. *Nat Cell Biol* 3: 114-20.
- TADDEI, A., ROCHE, D., BICKMORE, W.A. and ALMOUZNI, G. (2005). The effects of histone deacetylase inhibitors on heterochromatin: implications for anticancer therapy? *EMBO Rep* 6: 520-4.
- TOTH, K.F., KNOCH, T.A., WACHSMUTH, M., FRANK-STOHR, M., STOHR, M., BACHER, C.P., MULLER, G. and RIPPE, K. (2004). Trichostatin A-induced histone acetylation causes decondensation of interphase chromatin. *J Cell Sci* 117: 4277-87.
- UNGERSTEDT, J.S., SOWA, Y., XU, W.S., SHAO, Y., DOKMANOVIC, M., PEREZ, G., NGO, L., HOLMGREN, A., JIANG, X. and MARKS, P.A. (2005). Role of thio-redoxin in the response of normal and transformed cells to histone deacetylase inhibitors. *Proc. Natl. Acad. Sci. USA* 102: 673-678.
- VAN DEN BERG, I.M., ELEVELD, C., VANDERHOEVEN, M., BIRNIE, E., STEEGERS, E.A.P., GALJAARD, R.J., LAVEN, J.S.E. and VANDOORNINCK, J.H. (2011). Defective deacetylation of histone 4 K12 in human oocytes is associated with advanced maternal age and chromosome misalignment. *Hum. Reprod.* 26: 1181-1190.
- WICKRAMASINGHE, D., EBERT, K.M. and ALBERTINI, D.F. (1991). Meiotic competence acquisition is associated with the appearance of M-phase characteristics in growing mouse oocytes. *Dev. Biol.* 143: 162-172.
- YANG, F., BAUMANN, C. and DE LA FUENTE, R. (2009). Persistence of histone H2AX phosphorylation after meiotic chromosome synapsis and abnormal centromere cohesion in poly (ADP-ribose) polymerase (Parp-1) null oocytes. *Dev Biol* 331: 326-338.
- YU, H.G. and KOSHLAND, D. (2005). Chromosome morphogenesis: condensin-dependent cohesin removal during meiosis. *Cell* 123: 397-407.
- ZUCCOTTI, M., PICCINELLIA, ROSSI PG, GARAGNAS, REDICA. (1995). Chromatin organization during mouse oocyte growth. *Mol Reprod Dev* 4: 479-85.

Further Related Reading, published previously in the *Int. J. Dev. Biol.*

Impaired meiotic competence in putative primordial germ cells produced from mouse embryonic stem cells

Marianna Tedesco, Donatella Farini and Massimo De Felici
Int. J. Dev. Biol. (2011) 55: 215-222

Chemical genomics: a key to the epigenome - An interview with Minoru Yoshida

Saadi Khochbin
Int. J. Dev. Biol. (2009) 53: 269-274

Epigenetic asymmetry in the zygote and mammalian development

Robert Feil
Int. J. Dev. Biol. (2009) 53: 191-201

Dynamic distribution of the replacement histone variant H3.3 in the mouse oocyte and preimplantation embryos

Maria-Elena Torres-Padilla, Andrew J. Bannister, Paul J. Hurd, Tony Kouzarides and Magdalena Zernicka-Goetz
Int. J. Dev. Biol. (2006) 50: 455-461

X-chromosome activity: impact of imprinting and chromatin structure

R V Jamieson, P P Tam and M Gardiner-Garden
Int. J. Dev. Biol. (1996) 40: 1065-1080

5 yr ISI Impact Factor (2011) = 2.959

